Heliyon 10 (2024) e32109

Contents lists available at ScienceDirect

Heliyon

journal homepage: www.cell.com/heliyon

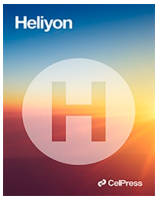

Research article

Comparative assessment of emissions, performance, and economics parameters for a dual–fuel diesel generator operating with rice bran biodiesel and hydrogen

Raquel Laguado-Ramírez [a], Fanny Hernandez-Villamizar [a], Jorge Duarte-Forero [b,*]

[a] GIINGPRO Research Unit, Programa de Ingeniería Industrial, Universidad Francisco de Paula Santander, Avenida Gran Colombia No. 12E-96 Colsag, San José de Cúcuta, 540001, Norte de Santander, Colombia
[b] KAI Research Unit, Department of Mechanical Engineering, Universidad del Atlántico, Carrera 30 Número 8–49, Puerto Colombia, 081001, Atlántico, Colombia

ARTICLE INFO

Keywords:
Combustion engine
Dual
Fuel
Efficiency
Emissions
Hydrogen
Rice bran

ABSTRACT

The first step to achieving an energy transition is partially substituting fossil fuels with other more environmentally friendly alternatives, such as hydrogen gas. The current research aims to evaluate the influence of hydrogen in a diesel generator fueled with rice bran biodiesel. The above encourages the use of hydrogen and biodiesel production from residual raw material. For the development of the research, a diesel engine bench was used, which operated in five load conditions: 20 %, 40 %, 60 %, 80 %, and 100 %, and was fed with three fuels: −100 %, RB-10 %, and RB-10 % + H_2(30 %). The results show that the mixture RB-10 % + H_2(30 %) causes a 3.14 % reduction in BSFC and a 3.26 % increase in energy conversion efficiency. In addition, it is observed that a 9.90 %, 12.57 %, and 10.99 % decrease in HC, CO, and smoke opacity emissions compared to pure diesel. On the other hand, the mixture RB-10 % + H_2(30 %) reduces by 4.44 %, 5.07 %, and 7.06 % the environmental, social, and ecological impact due to CO_2, HC, and CO emissions, as well as a 3.93 % reduction in engine operating cost compared to RB-10 % biodiesel. In general, hydrogen injection is a promising alternative to promote the use of rice bran biodiesel due to its increased performance characteristics and reduced pollutant emissions without the need to modify the engine.

Nomenclature

ICE	Internal combustion engine [−]
CO	Carbon monoxide [g/kWh]
CO2	Carbon dioxide [g/kWh]
NO	Nitric oxide [−]
NO2	Nitrogen dioxide [−]
NOx	Nitrogen oxides [g/kWh]
HC	Hydrocarbons [g/kWh]
RB	Rice bran biodiesel [−]
HEF	Hydrogen energy fraction [%]
$\dot{m}$	Fuel mass flow [g/s]

(*continued on next page*)

* Corresponding author.
E-mail address: jorgeduarte@mail.uniatlantico.edu.co (J. Duarte-Forero).

https://doi.org/10.1016/j.heliyon.2024.e32109
Received 30 March 2024; Received in revised form 11 May 2024; Accepted 28 May 2024
Available online 29 May 2024

(*continued*)

LHV	lower heating value [MJ/kg]
$u(x)$	Uncertainty
HRR	Heat release rates [J/°]
Q_w	Heat loss through [J]
$\dot{m}_{bb}$	Blow-by flow rate [g/s]
c_v	Specific heat (constant volume) [J/(kg K)]
R	Exhaust gas constant [J/K mol)]
$\dot{m}_f$	Fuel injected rate [g/s]
V	Instantaneous cylinder volume [m^3]
p	Pressure [bar]
T	Temperature [K]
u	Internal energy [J]
$h_{f(l),iny}$	Enthalpy [J]
A_p	Gap area [m^2]
k	Ratio of specific heat capacities [J/(kg K)]
p_c	Crankcase pressure [bar]
c_{bb}	Discharge coefficient [−]
r_c	Volumetric compression ratio [−]
l_b	Connecting rod length [m]
l_c	Crankshaft length [m]
E_s	Elastic modulus [Pa]
m_i	Inertial mass [m]
k_d	Mechanical deformation [−]
a_p	Piston acceleration [m^2/s]
R_p	Piston vertical position [m]
A_p	Piston area [m^2]
A_s	Total heat loss surface [J]
T_w	Cylinder wall temperature [T]
h	Heat transfer coefficient [J/(m^2 K)]
$\dot{E}_i$	Energy [J]
BSFC	Brake specific fuel consumption [g/kWh]
BTE	Brake thermal efficiency [%]
ESC_i	Environmental and social impact cost [USD/kWh]
EC_i	Ecological cost [USD/kWh]
C_w	Cost of useful work [USD/kWh]
C_ψ	Cost of exergy loss [USD/kWh]
C_{fuel}	Price of the fuel [USD/J]
c_f	Engine cost [USD]
e_f	Capital factor of the investment [−]
t_p	Operating time per year [h]
M_f	Engine maintenance factor [−]
n	Engine lifetime [year]
i	Interest rate [−]
Greek symbols	
ω	Rotational speed
θ	Crankshaft angle
$\dot{\psi}_i$	Exergy
Γ	Torque
φ	Factor exergy
ρ	Density
ζ	price of fuel per cubic meter
Subscripts	
l	Liquid fuel
g	Gaseous fuel
i	Input
exh	Exhaust gases

1. Introduction

One of the main concerns of the last decade is the depletion of fossil resources and the continuous increase of polluting emissions, which cause global warming and climate change [1]. This situation has promoted the constant search for renewable, ecological, and sustainable fuel sources [2]. Currently, internal combustion engines (ICE) are used in many activities in the agricultural, industrial, and transportation sectors [3]. The main fuel used is diesel, which is derived from petroleum products and is therefore harmful to the environment [4]. To solve this problem, alternative such as biodiesel and hydrogen have been proposed to replace or partially substitute petroleum products [5]. Studies indicate that biodiesel is possibly the most viable option to reduce the environmental impact of ICEs because it does not require modifications for its implementation [6].

Biodiesel has several advantages that motivate its use in internal combustion engines. The first is its environmental friendliness due to its degradability and non-toxicity characteristics [7]. The second advantage is its ability to be produced with many raw materials,

such as animal fats and vegetable oils, making it a sustainable fuel. Finally, the physicochemical properties of biodiesel are very similar to pure diesel, and it can be mixed directly with diesel without significant modifications in the injection and fuel supply system [8]. Feedstock sources for biodiesel production include using seeds such as palm, sunflower, peanut, soybean, rapeseed, cottonseed, and rice bran [9]. Among the options available for biodiesel production, rice bran stands out for its easy accessibility, non-toxicity, natural availability, and sustainability [10]. Despite the advantages of biodiesel, it presents several drawbacks due to high viscosity and density, which cause less efficient fuel pulverization. Additionally, biodiesel has a lower calorific value than pure diesel [11]. These characteristics discourage the use of this alternative fuel.

In recent years, hydrogen has gained high interest for its great potential to achieve an energy transition due to the absence of carbon in its nuclear structure. This makes it a promising fuel for reducing greenhouse gas emissions. In addition, hydrogen is characterized by its high diffusivity, flame speed, and high calorific value. However, hydrogen cannot be used directly in diesel engines. This limitation is associated with the lower ignition energy of hydrogen, which is lower than fuels derived from petroleum. This can lead to spontaneous ignition of hydrogen before the compression stage, resulting in abnormal phenomena during combustion that affect the safety and performance of the engine [12]. Dual fuel mode is the best way to use hydrogen in internal combustion engines. This involves the injection of the gaseous fuel (hydrogen) through the intake air manifold, which is then burned in the cylinder chamber together with the liquid fuel (pure diesel or biodiesel) [13].

In the literature, several studies have analyzed the effect of hydrogen injection on engines fueled with biodiesel from different feedstocks [10]. Gnanamoorthi and Vimalananth [14] studied the influence of hydrogen in a direct-injection diesel engine. The conclusions obtained indicate that adding a volumetric flow of 30 lpm causes a decrease in exhaust emissions and an improvement in efficiency. Jamrozik et al. [15] evaluated an engine's stability, emissions, and performance with hydrogen injection. The results show that adding hydrogen with an energy fraction of 25 % does not cause problems in the stability of the engine. Mejia et al. [16] implemented mathematical correlations to estimate CO, CO_2, NO, NO_2, and NOx emissions in a diesel engine fueled with different blends of African palm oil biodiesel: B5 and B10. A process to help with engine calibration and optimization is obtained from the maps developed.

Mendoza et al. [17] studied the influence of hydroxy with biodiesel produced from microalgae and Karanja. The results show that the addition of hydroxy is a promising alternative to reduce pollutant emissions and improve engine efficiency. Forero et al. [18] evaluated a low-displacement diesel engine fueled with hydroxy gas and biodiesel from palm oil residues. The conclusions indicate a 9.39 % and 11.02 % decrease in smoke and hydrocarbon opacity.

Loganathan et al. [19] used mixtures of diesel and hydrogen in an internal combustion engine. The trends obtained indicate a decrease in CO and HC emissions. Akar et al. [20] tested different hydrogen flow rates with biodiesel mixtures in an IC engine. The research shows a 62.5 % decrease in CO emissions. Additionally, a slight increase in efficiency and a 1.66 % reduction in diesel fuel consumption were obtained. Kuntang et al. [21] investigated different hydrogen flows (2.5, 5, 7.5, and 10 lpm) mixed with palm oil biodiesel. The results indicated a 27.38 % increase in thermal efficiency and a 47.61 % decrease in specific fuel consumption compared to biodiesel. Zhang et al. [22] studied 10 %, 20 %, and 30 % biodiesel mixtures with a hydrogen volumetric flow rate of 10 lpm. The addition of biodiesel and hydrogen in diesel reduced carbon dioxide, hydrocarbons, nitrogen oxides, and carbon monoxide emissions. Ravikumar [23] investigated the use of sapote seeds for biodiesel production running on a mixture of hydrogen gas (3 and 6 lpm). The trends obtained indicate an increase in cylinder pressure of 17.26 % and heat release rate of 43.91 %. Additionally, a reduction of 18.61 %, 49.68 %, 63.01 %, and 23.24 % in carbon dioxide, carbon monoxide, hydrocarbon, and smoke opacity emissions were reported. Tan et al. [24] analyzed the emission, performance, and combustion characteristics of a marine engine fueled with rapeseed methyl ester, water, and hydrogen with 5 %, 10 % and 15 % energy fraction. The research demonstrates that water and hydrogen allow for improved combustion characteristics and emissions of the marine engine. Mohite et al. [25] studied the improvement of emissions and performance of a dual-fuel (biodiesel - hydrogen) engine using a response surface methodology. A 12.12 % and 36.13 % reduction in CO and HC emissions was observed.

In Colombia, rice cultivation has a high participation due to its enormous extension of harvested area. Rice is the third largest agricultural crop, using 13 % of the country's harvested area. In addition, rice production represents 6 % of agricultural production and 10 % of agricultural activities [26]. Because it is a foodstuff for mass consumption, the industrialization of rice leads to the generation of a large amount of waste by-products. Two by-products are produced during rice milling: rice peel and rice bran. This residual matter is equivalent to 25 % and 10 % of the weight of the unpeeled grain [27]. Rice by-products can negatively affect the environment. The high availability of rice bran in Colombia makes it a low-cost raw material, making it an attractive product to use in biodiesel production.

The rice industry in Colombia produces approximately 400,000 tons of rice bran waste, of which 15 % is used as fuel material during the rice drying process [28]. The remaining percentage is incinerated and dumped into the environment. Rice bran residues increase operational costs due to transporting them to incineration centers. Additionally, this waste is characterized by a low natural degradability, making it prone to accumulating in the environment causing extreme pollution, especially in water sources. When rice bran is incinerated in the open air, it causes an adverse alteration of the soil's physical, chemical, and biological conditions. In addition, the emissions generated can cause respiratory diseases.

On the other hand, rice bran contains a high silica content, resulting in decreased digestibility. This limits the use of this product in the food processing field. The few alternatives for using rice bran encourage the country's producers and millers to use incineration techniques in open fields. Therefore, it is necessary to propose projects that promote using this raw material to reduce its environmental impact and improve the country's economic sector.

Studies described in the literature indicate that hydrogen can improve the characteristics of biofuels from various feedstocks. These include improvements in thermal efficiency and engine fuel consumption. As well as reductions in carbon dioxide, hydrocarbon, and

carbon monoxide emissions [29]. The influence of hydrogen in biofuel depends mainly on the chemical composition of the feedstock used. The literature shows that little research has been carried out with this feedstock in the case of mixtures of rice bran biodiesel and hydrogen. Additionally, the studies conducted are focused only on performance parameters such as BTE and BSFC and emission characteristics such as CO, CO2, HC, and smoke opacity [30,31]. Other key factors, such as combustion characteristics, thermodynamic balances, operational costs, and social and environmental impact, have not been discussed in the literature.

In the present study, an analysis of the use of rice bran to produce biodiesel and its behavior when used in dual fuel with hydrogen is carried out. A diesel engine generator bank was used for the research development, and five load conditions were established: 20 %, 40 %, 60 %, 80 %, and 100 %. The engine was fueled with three types of fuels: pure diesel (D-100 %), rice bran biodiesel (RB-10 %), and biodiesel-hydrogen mixture (RB-10 % + H_2(30 %)). The analysis will be focused on evaluating the performance parameters, energy and exergy balance, emission levels, and influence on the engine's operating costs. In this way, we encourage using rice bran produced in Colombia to prepare biodiesel, which can later be used in the country's transportation sector. With the development of this research, an innovative solution is proposed for the use of rice bran waste material from rice mills in Colombia, which has not been evaluated before. In this way, it seeks to reduce environmental pollution and the adverse effects on human health caused by the poor management of rice bran waste. Additionally, this contributes to the literature with research focused on deepening the influence of hydrogen in rice bran biodiesel through analyses involving combustion characteristics, thermodynamic balances, operational costs, and social and environmental impact.

2. Fuel properties

A two-stage transesterification process obtained rice bran bio-oil. During the first step, catalyzed transesterification is performed, adding crude rice bran oil to a conical flask. This oil was subjected to a preheating process for 30 min at a temperature of 60 °C. In the second step, an amount of alcohol (methanol) and a catalyst (sulfuric acid) were added to the preheated oil. The mixture obtained was stirred at constant speed for 60 min and maintained at a temperature of 60 °C through a water bath. In the third step, the Impurities in the mixture were removed using a separating funnel. During the fourth step, the obtained oil is heated to a temperature of 60 °C and mixed with alcohol (methanol) and base catalyst (potassium hydroxide). The mixture obtained underwent a stirring process at a constant speed for 60 min and maintained a temperature of 60 °C. In the fifth step, the settled glycerol was separated and removed from the mixture through a separating funnel. Finally, in the sixth step, the rice bran bio-oil was purified by washing and drying to eliminate water, methanol, and potassium hydroxide challenges. The product obtained was used to prepare a blend of rice bran biodiesel identified as RB-10 % (90 % diesel and 10 % rice bran bio-oil). The engine used for the experimental tests was also fueled with pure diesel (D-100 %) and hydrogen gas (H_2). The physicochemical characteristics of the fuels used are shown in Table 1.

3. Experimental methodology

The experimental test engine configuration is indicated in Fig. 1. A single-cylinder, 4-stroke, direct injection, naturally aspirated diesel engine was used in the present investigation.

In the test bench, a liquid fuel feeding system with measurement and a hydrogen feeding system is available, along with its security system (flame arrester) and filtering. The engine receives load from a resistive load bank.

Table 2 shows the technical specifications of the engine. Hydrogen was added to the engine through the air intake pipe. A pressure regulator and a volumetric flow meter were used to control hydrogen gas's injection pressure and flow rate. The addition of hydrogen gas was determined using an energy fraction of 30 %, calculated by equation (1).

$$HEF = \frac{\dot{m}_g \times LHV_g}{\left(\dot{m}_g \times LHV_g\right) + \left(\dot{m}_l \times LHV_l\right)} \tag{1}$$

where *LHV* is the lower heating value. The subscripts *l* and *g* refer to liquid fuel (diesel or biodiesel) and gaseous fuel (gas hydrogen) [30,31]. As safety measures, a flame arrester and a silica gel filter were installed to prevent flame backflow and protect the hydrogen storage tank. The engine is operated at a constant rotation speed of 3600 rpm, and five load conditions (20 %, 40 %, 60 %, 80 %, and 100 %). In each experimental test a time of 10 min was set to ensure a steady state condition. Additionally, an average reading was used by repeating each test three times.

The engine's speed was measured by a crank angle sensor (Beck Arnley 180–0420). A mass flow sensor (BOSCH 22680 7J600) was used to determine the intake airflow. The pressure in the cylinder chamber was determined using a piezoelectric transducer (KISTLER type 7063-A). Fuel consumption was calculated using a stopwatch and a precision balance (OHAUS PA313). The operational

Table 1
Physicochemical properties of rice bran biodiesel, diesel, and hydrogen.

Property	Unit	Value		
		Diesel (D-100 %)	Rice bran biodiesel (RB-10 %)	Hydrogen (H_2)
Density	kg m^{-3}	850	853	0.08376
Kinematic viscosity	mm^2 s^{-1}	3.12	3.46	[–]
Flash point	°C	76	90	[–]
Lower heating value	MJ kg^{-1}	42.3	41.7	120.21

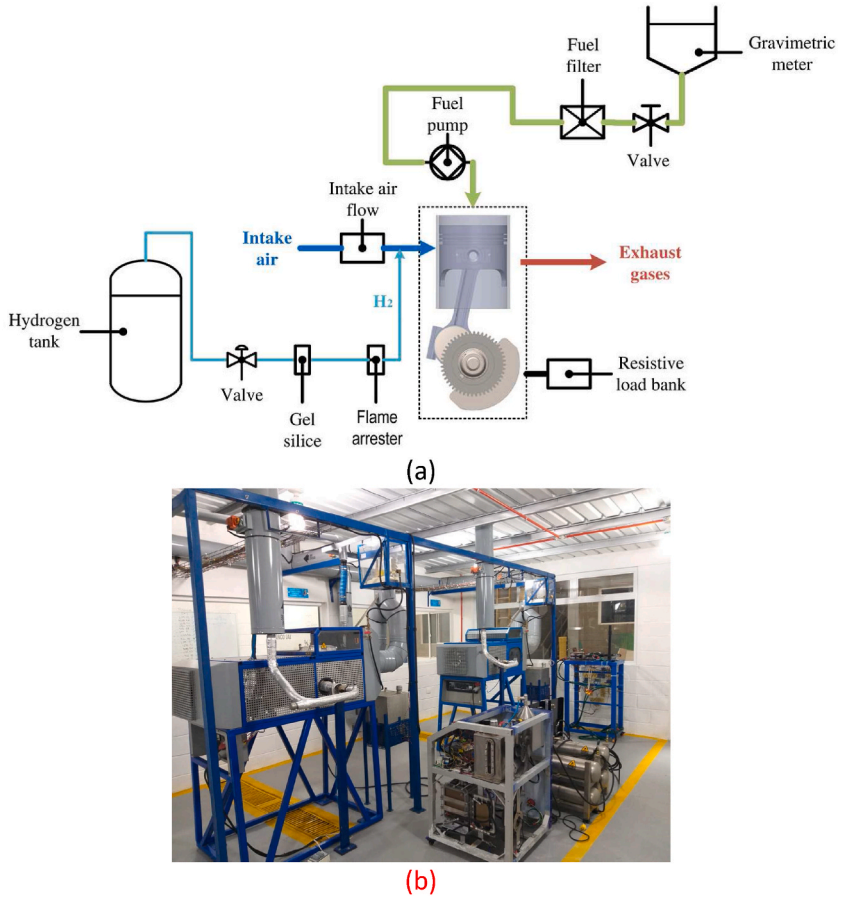

Fig. 1. (a) Schematic experimental configuration, and (b) diesel engine test bench.

Table 2
Specifications of the experimental test engine.

Engine parameter	Specifications
Engine type	SOKAN - MDF300
Number of cylinders	1
Bore [mm]	78
Number of cycles	Four – stroke
Stroke [mm]	63
Intake system	Naturally aspirated
Cooling type	Air-cooled
Injection system	Direct injection
Volume [cc]	300

temperature of the engine was measured using K-type thermocouples. Two exhaust gas analyzers (PCA® 400 and Brain Bee AGS-688) and an opacimeter (Brain Bee OPA-100) were used to measure emission levels. The technical characteristics of the instruments are shown in Table 3.

Experimental test measurements are subject to uncertainty due to instrument calibration, human error, and environmental conditions. All these factors cause an error in the measurement. To ensure the measurements' reliability, the uncertainty was calculated using the type A evaluation, which is based on a statistical analysis of a series of observations. The experimental uncertainty (u) of an average value was calculated using equation (2).

$$u_{(x)} = \sqrt[2]{\sum_{i=1}^{n} \frac{(\overline{x} - x_i)^2}{n \times (n-1)}} \tag{2}$$

where n is the number of measurements of a variable $(n = 3)$. $\overline{x}$ is the average of a series n of measurements, which is resolved by

Table 3
Measurement range and uncertainty of the measuring instruments.

Variable	Unit	Measuring instrument	Range		Uncertainty (%)
			Max.	Min.	
Intake air mass flow	g/s	BOSCH 22680 7J600	0	125	±1.2
NOx	ppm	PCA® 400	0	3000	±1.1
Temperature	°C	Thermocouple Type K	−200	1370	±0.5
rpm	RPM	Beck Arnley 180 0420	5	9999	±0.5
Mass	g	OHAUS PA313	0	310	±0.6
Pressure	bar	Piezoelectric transducer	0	250	±0.5
HC	ppm	Brain Bee AGS 688	0	20	±1.0
CO	vol%		0	10	±0.5
CO_2	vol%		0	20	±1.0
Smoke opacity	%	Brain Bee OPA 100	0	99.9	±1.2

equation (3).

$$\overline{x} = \sum_{i=1}^{n} \frac{x_i}{n} \tag{3}$$

The value of the measurement, considering its uncertainty, is represented in equation (4).

$$y = \overline{x} \pm u_{(x)} \tag{4}$$

Combined uncertainty was used in the case of variables that depend on more than one measurement, which allows for the combination of all uncertainty components [32]. Table 4 shows the calculation of combined uncertainty for the main variables analyzed in the research.

4. Results and discussion

4.1. Analysis of combustion characteristics

A model was developed to observe changes in heat release rates in order to investigate the combustion process. The engine combustion chamber was treated as an open system [33,34]. The model formulation incorporated several considerations: (1) maintaining a constant pressure inside the combustion chamber, justified by the significantly slower fluid and combustion flame propagation velocities compared to the velocity of sound [35], (2) modeling the gases inside the chamber as ideal gases [36], (3) accounting for the specific heat of the gases based solely on chemical composition and temperature, (4) stoichiometric calculation of the combustion products [37], (5) determining thermodynamic properties using the average combustion chamber temperature, (6) incorporating heat transfer through the deformations of the piston mechanism and cylinder walls, and (7) determining heat transfer coefficients through Woschni correlations [38]. Equation (5) illustrates the combustion model derived from the principles of the first law of thermodynamics [39].

Table 4
Calculation of combined uncertainty.

Variable	Nomenclature	Unit	Combined uncertainty
Shaft energy	$\dot{E}_s$	kW	$u_{(\dot{E}_s)} = \sqrt{\left(u_{(\omega)} \times \frac{\dot{E}_s}{\omega}\right)^2 + \left(u_{(\Gamma)} \times \frac{\dot{E}_s}{\Gamma}\right)^2}$
Fuel consumption	$\dot{m}_{fuel}$	g/s	$u_{(\dot{m}_{fuel})} = \sqrt{\left(u_{(\dot{m}_l)} \times \frac{\dot{m}_{fuel}}{\dot{m}_l}\right)^2 + \left(u_{(\dot{m}_g)} \times \frac{\dot{m}_{fuel}}{\dot{m}_g}\right)^2}$
Brake specific fuel consumption	$BSFC$	g/kWh	$u_{(BSFC)} = \sqrt{\left(u_{(\omega)} \times \frac{BSFC}{\omega}\right)^2 + \left(u_{(\Gamma)} \times \frac{BSFC}{\Gamma}\right)^2 + \left(u_{(\dot{m}_{fuel})} \times \frac{BSFC}{\dot{m}_{fuel}}\right)^2}$
Brake thermal efficiency	BTE	%	$u_{(BTE)} = \sqrt{\left(u_{(\omega)} \times \frac{BTE}{\omega}\right)^2 + \left(u_{(\Gamma)} \times \frac{BTE}{\Gamma}\right)^2 + \left(u_{(\dot{m}_{fuel})} \times \frac{BTE}{\dot{m}_{fuel}}\right)^2}$
Carbon dioxide	CO_2	g/kWh	$u_{(CO_2)} = \sqrt{\left(\frac{u_{(CO_2)}}{CO_2}\right)^2 + \left(\frac{u_{(\dot{E}_s)}}{\dot{E}_s}\right)^2}$
Hydrocarbons	HC	g/kWh	$u_{(HC)} = \sqrt{\left(\frac{u_{(HC)}}{HC}\right)^2 + \left(\frac{u_{(\dot{E}_s)}}{\dot{E}_s}\right)^2}$
Nitrogen oxides	NO_x	g/kWh	$u_{(NO_x)} = \sqrt{\left(\frac{u_{(NO_x)}}{NO_x}\right)^2 + \left(\frac{u_{(\dot{E}_s)}}{\dot{E}_s}\right)^2}$
Carbon monoxide	CO	g/kWh	$u_{(CO)} = \sqrt{\left(\frac{u_{(CO)}}{CO}\right)^2 + \left(\frac{u_{(\dot{E}_s)}}{\dot{E}_s}\right)^2}$

$$HRR = \frac{dQ_w}{d\theta} + RT\frac{d\dot{m}_{bb}}{d\theta} + m_c c_v \frac{dT}{d\theta} - \left(h_{f(l),iny} - u\right)\frac{d\dot{m}_f}{d\theta} + p\frac{dV}{d\theta} \tag{5}$$

where Q_w is the heat loss, $\dot{m}_{bb}$ is the blow-by flow rate, c_v is the specific heat at constant volume, R is the exhaust gas constant, $\dot{m}_f$ is the fuel injected rate, V is the instantaneous cylinder volume, p is the instantaneous cylinder pressure, T is the temperature, θ is the crankshaft angle, m_c is the amount of gas in the cylinder, u is the internal energy, and $h_{f(l),iny}$ is the enthalpy of the fuel injected, respectively.

The blow-by flow rate ($\dot{m}_{bb}$) was represented as a compressible flow process, as shown in equation (6) [40,41].

$$\dot{m}_{bb} = \begin{cases} \dfrac{c_{bb}A_r p}{\sqrt{RT}} k^{1/2}\left(\dfrac{2}{k+1}\right)^{\frac{k+1}{2(k-1)}} & , \dfrac{p_c}{p} \le \left(\dfrac{2}{k+1}\right)^{\frac{k}{k-1}} \\ \left[\dfrac{2k}{k-1}\left(\left(\dfrac{p_c}{p}\right)^{\frac{2}{k}} - \left(\dfrac{p_c}{p}\right)^{\frac{k+1}{k}}\right)\right]^{1/2} & , \dfrac{p_c}{p} > \left(\dfrac{2}{k+1}\right)^{\frac{k}{k-1}} \end{cases} \tag{6}$$

where A_r is the gap area, k is the ratio of specific heat capacities, p_c is the crankcase pressure and c_{bb} is the discharge coefficient, respectively. The instantaneous cylinder volume (V) is determined using equation (7).

$$V = \frac{\pi d^2}{4}\left(\frac{2l_c}{r_c - 1}\right) + \frac{\pi d^2}{4}\left(l_c + l_b - R_p\right) + \frac{\pi d^2}{4}\frac{k_d l_b\left(pA_p + m_i a_p\right)}{E_s} \tag{7}$$

where r_c is the volumetric compression ratio, l_b is the connecting rod length, l_c is the crankshaft length, E_s is the elastic modulus, m_i is the inertial mass, k_d is the mechanical deformation, a_p is the piston acceleration, R_p is the vertical position of the piston, and A_p is the piston area, respectively. The heat loss through the combustion chamber walls (Q_w) was calculated by equation (8).

$$Q_w = h \times A_s \times (T - T_w) \tag{8}$$

where A_s is the total heat loss surface, T_w is the cylinder wall temperature, and h is the heat transfer coefficient, respectively. Equations (9) and (10) were used to calculate the temperature (T) and rate of temperature change ($dT/d\theta$) inside the combustor.

$$T = \frac{pV}{m_c R} \tag{9}$$

$$\frac{dT}{d\theta} = \frac{-p\frac{dV}{d\theta} - \frac{dQ_w}{d\theta} - \frac{d\dot{m}_{bb}}{d\theta}RT}{m_c c_v} \tag{10}$$

Fig. 2 shows the variation of cylinder chamber pressure when the engine is fueled with diesel (D-100 %), biodiesel (RB-10 %), and the biodiesel-hydrogen mixture (RB-10 % + H_2(30 %)).

The curves shown in Fig. 2 correspond to a load percentage of 100 %. The results indicate that adding hydrogen causes an increase in the maximum combustion pressure. The maximum pressure levels reached were 67.30 bar, 62.05 bar, and 64.56 bar for D-100 %, RB-10 %, and RB-10 % + H_2(30 %), respectively. Rice bran biodiesel reduces the combustion pressure by 7.80 % due to the lower calorific value of RB-10 % compared to pure diesel. However, hydrogen presents a calorific value approximately three times higher than D-100 % fuel. This allows the mixture of biodiesel enriched with hydrogen (RB-10 % + H_2(30 %)) to increase the peak pressure by 4 % compared to RB-10 %. Additionally, the hydrogen content causes an increase in flame propagation speed and combustion velocity. Both result in a faster combustion process, resulting in a higher heat release and, therefore, an increase in cylinder pressure. Similar studies have observed that adding hydrogen tends to improve the combustion process, evidenced by a higher peak pressure [41].

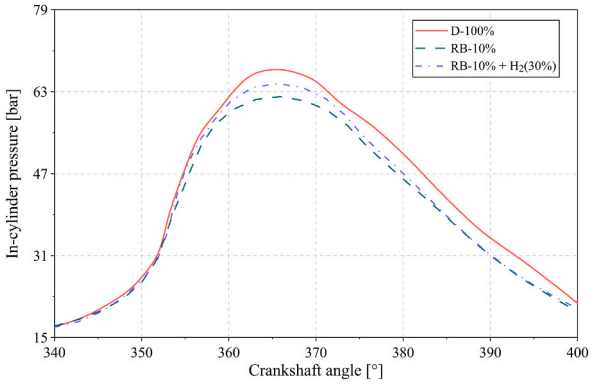

Fig. 2. Cylinder pressure variation for different fuels.

The addition of hydrogen in the engine also significantly impacts the heat release rate, as shown in Fig. 3.

The results obtained indicate that diesel fuel has the highest heat release rate (24.30 J/deg), followed by the mixture RB-10 % + H_2(30 %) (23.39 J/deg) and rice bran biodiesel (21.99 J/deg). The reduction of HHR in rice bran biodiesel is associated with slower combustion velocity and increased viscosity since the heat release is strongly related to the velocity of the air/fuel mixture [42]. The heat release rate depends mainly on the fuel's calorific value and the air-fuel mixture's homogeneity. These factors are improved with hydrogen injection in biodiesel due to its higher calorific value, high diffusivity, and hydrogen flame speed. The RB-10 % biodiesel presents a 9.53 % reduction in the maximum level of heat release rate. However, with the mixture RB-10 % + H_2(30 %), an increase of 6.40 % is achieved.

4.2. Energy balance and exergy analysis

The test engine is considered a stationary system with an open control volume to analyze the energy and exergy distribution. The equations used to determine the energy and exergy parameters are shown in Table 5.

Fig. 4 shows the energy distribution for the different fuels and engine load conditions: shaft energy, exhaust gas energy, and energy loss.

From the results obtained, it can be observed that the conversion of chemical energy of the fuel to useful energy (mechanical power) increases as a function of the higher workload of the engine. This result is evident in all the fuels used to feed the engine, which implies a low energy efficiency for low load conditions. The variation of energy conversion efficiency was 9.64–30.38 %, 9.23–28.52 %, and 9.54–29.98 % for D-100 %, RB-10 % and RB-10 % + H_2(30 %), respectively. The calorific value of the fuel has a direct influence on the energy conversion efficiency of the engine. This causes rice bran biodiesel to present an average reduction of 4.24 % compared to pure diesel. However, with the help of hydrogen, the mixture RB-10 % + H_2(30 %) increases the engine performance by 3.26 % compared to RB-10 % biodiesel.

Much of the fuel's chemical energy is converted into energy loss due to heat generated, friction, auxiliary system power, and combustion inefficiency. This becomes especially significant at low load conditions. For a load percentage of 20 %, a maximum energy loss of 73.48 %, 72.40 % and 71.04 % is observed with D-100 %, RB-10 % and RB-10 % + H_2(30 %) fuel.

In addition, the results show that the exhaust gases have a high percentage of thermal energy, which increases as a function of the engine load. This is due to higher fuel injection, causing an increase in the exhaust gas temperature. The trends obtained indicate that RB-10 % and RB-10 % + H_2(30 %) fuel causes an average increase of 8.38 % and 14.83 % in the percentage of exhaust gas energy when compared to pure diesel. This can be attributed to an improvement in combustion homogeneity caused by the contribution of more oxygen content in rice bran biodiesel and a better air-fuel mixture caused by the velocity of hydrogen flame propagation.

To analyze the exergy distribution of the engine, the percentage of input exergy corresponding to shaft exergy, exhaust gas exergy, exergy loss, and exergy destruction is analyzed. The results obtained are shown in Fig. 5.

The shaft exergy indicates the percentage of input exergy that was converted into useful work, which allows for determining the exergy of the engine. This allows determining the exergy efficiency for different fuels and load conditions. The results show that the exergy efficiency varies between 9.00 and 28.34 %, 8.61 %–26.59 %, and 8.97–28.20 % for D-100 %, RB-10 %, and RB-10 % + H_2(30 %) fuel. The exergy efficiency levels were, on average, lower than the energy yield described in Fig. 4.

The exergy loss from the engine was approximately equal across all fuel types, with a variation of 4.58–7.03 %. This percentage of exergy is associated with heat transfer losses, especially due to the convection phenomenon between the engine body and the environment. In the case of the exhaust gas exergy, it was observed that it tends to increase with a higher percentage load on the engine due to the increase in the mass flow of the gases and the combustion temperature. For 100 % load, an exhaust gas exergy percentage of 10.68 %, 11.98 %, and 13.12 % is reported with D-100 %, RB-10 %, and RB-10 % + H_2(30 %) fuel. On average, rice bran biodiesel and the biodiesel-hydrogen mixture cause an increase of 13.55 % and 26.69 % in the percentage of exhaust gas exergy compared to pure diesel.

Much of the fuel input exergy is converted to exergy destruction, especially at low load conditions. These losses are a consequence

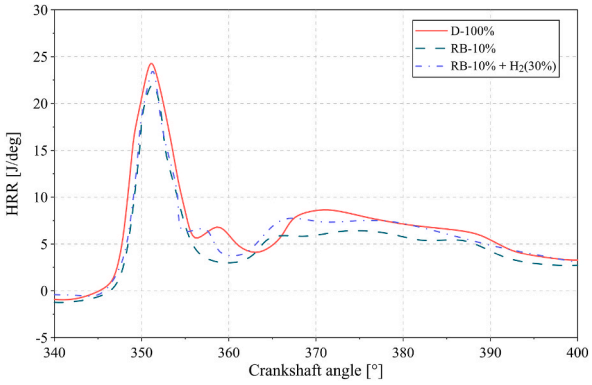

Fig. 3. Variation of heat release rate for different fuels.

Table 5
Energy and exergy calculation.

Description	Energy Analysis	Exergy Analysis
Input fuel energy	$\dot{E}_i = (\dot{m}_l \times LHV_l) + (\dot{m}_g \times LHV_g)$	$\dot{\psi}_i = \varphi_l(\dot{m}_l \times LHV_l) + \varphi_g(\dot{m}_g \times LHV_g)$
Exhaust gas energy	$\dot{E}_{exh} = \dot{m}_{exh} \times c_{p,T_{exh}} \times (T_{exh} - T_o)$	$\dot{\psi}_{exh} = \dot{m}_{exh} \times c_{p,T_{exh}} \times \left[(T_{exh} - T_o) - T_o \ln\left(\frac{T_{exh}}{T_o}\right)\right]$
Shaft energy	$\dot{E}_s = \frac{2\pi\omega \times \Gamma}{60}$	$\dot{\psi}_s = \dot{E}_s = \frac{2\pi\omega \times \Gamma}{60}$
Specific heat	$c_{p,T_{exh}} = (1.015580935928 \times 10^3) + (-1.512248401853 \times 10^{-1} \times T_{exh}) + (4.544870294058 \times 10^{-4} \times T_{exh}^2) + (-1.785063817167 \times 10^{-7} \times T_{exh}^3)$	
Energy loss	$\dot{E}_{loss} = \dot{E}_i - \dot{E}_s - \dot{E}_{exh}$	$\dot{\psi}_{loss} = \dot{E}_{loss}\left(1 - \frac{T_o}{T_s}\right)$
Exergy destruction	[−]	$\dot{\psi}_{dest} = \dot{\psi}_i - \dot{\psi}_s - \dot{\psi}_{exh} - \dot{\psi}_{loss}$
Efficiency	$\eta_e = \frac{\frac{2\pi\omega \times \Gamma}{60}}{(\dot{m}_l \times LHV_l) + (\dot{m}_g \times LHV_g)}$	$\eta_{exer} = \frac{\frac{2\pi\omega \times \Gamma}{60}}{\varphi_l(\dot{m}_l \times LHV_l) + \varphi_g(\dot{m}_g \times LHV_g)}$

of numerous internal irreversible processes, which are not directly quantified. For the engine used, an exergy destruction between 55.78 and 81.70 % was observed. Reducing exergy destruction would involve actions such as preheating the intake air, minimizing friction, improving thermal insulation, and reducing excess air.

4.3. Analysis of performance parameters

The brake specific fuel consumption (BSFC) is a performance parameter that measures the efficient use of fuel to produce useful work, which was calculated using equation (11).

$$BSFC = \frac{\dot{m}_{fuel}}{\frac{2\pi \times \omega \times \Gamma}{60}} \times 3600 \tag{11}$$

where $\dot{m}_{fuel}$ is the fuel flow, ω is the engine speed, and T is the torque, respectively. When the engine works in dual fuel mode, an equivalent fuel flow $(\dot{m}_{equiv})$ is used, as shown in equation (12).

$$\dot{m}_{equiv} = \dot{m}_{fuel} = \dot{m}_l + \frac{\dot{m}_g \times LHV_g}{LHV_l} \tag{12}$$

Fig. 6 shows the variation of BSFC for different fuels and engine load conditions.

The results show that the BSFC tends to decrease with increasing load. This indicates a higher amount of fuel consumption when the engine is running at low load percentages, which is evidence of poor combustion efficiency under these operating conditions. Although biodiesel favors complete combustion due to its higher oxygen content, its lower calorific value causes a 5.94 % increase in BSFC compared to pure diesel. Additionally, the higher density and viscosity of rice bran biodiesel reduces the efficiency of the atomization process, resulting in more fuel being injected. This implies a higher fuel demand to achieve the same mechanical power output. However, the mixture RB-10 % + H_2(30 %) allows a 3.14 % reduction in BSFC compared to rice bran biodiesel. This result is a combination of several factors, such as the high calorific value of hydrogen, the high flame speed, and its high flammability. In general, previous studies indicate a reduction in BSFC by adding hydrogen [43].

The brake thermal efficiency (BTE) of the engine was calculated using equation (13).

$$BTE = \frac{\frac{2\pi \times \omega \times \Gamma}{60}}{(\dot{m}_l \times LHV_l) + (\dot{m}_g \times LHV_g)} \times 100 \tag{13}$$

Fig. 7 shows the variation of BTE with the different fuel samples and load conditions. BTE tends to increase in relation to the engine load, which is a consequence of a more efficient combustion process. The maximum BTE was obtained at the highest load percentage with a value of 30.38 %, 28.52 %, and 29.98 % for D-100 %, RB-10 %, and RB-10 % + H_2(30 %) fuels, respectively. In general, it is observed that rice bran biodiesel reduces engine performance because of the lower calorific value and the lower atomization efficiency of the fuel due to its higher density and viscosity. These negative factors are partially solved with the addition of hydrogen. The mixture RB-10 % + H_2(30 %) causes a 3.26 % increase in BTE compared to RB-10 %.

The addition of hydrogen can minimize combustion problems associated with rice bran biodiesel. The combination of hydrogen and biodiesel through dual fuel allows for a better air-fuel mixture and a reduction in the amount of unburned fuel. Because the hydrogen is introduced into the intake manifold, there is sufficient time to achieve a homogeneous mixture. Additionally, the high diffusivity of hydrogen also favors homogeneity. Observations described in the literature show that hydrogen induction improves the BTE compared to the base fuel [41].

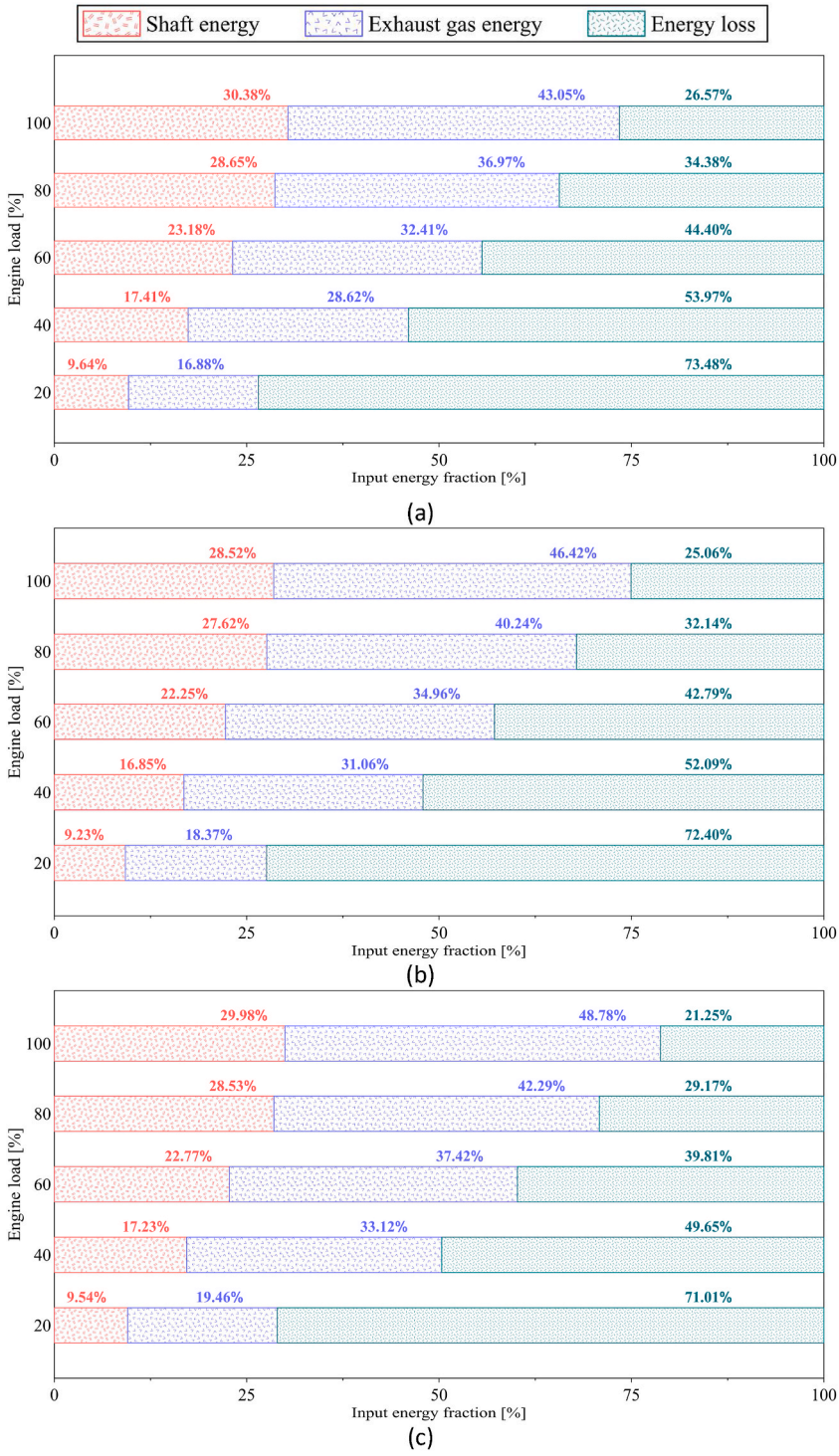

Fig. 4. Energy distribution for fuel (a) D-100 %, (b) RB-10 % and (c) RB-10 % + H_2(30 %).

4.4. Exhaust gas emissions analysis

Carbon dioxide (CO_2) emissions are a consequence of a complete combustion process. The CO_2 measurements obtained are shown in Fig. 8.

CO_2 emissions tend to increase with a higher percentage of engine load, resulting from increased fuel burn. The results show that

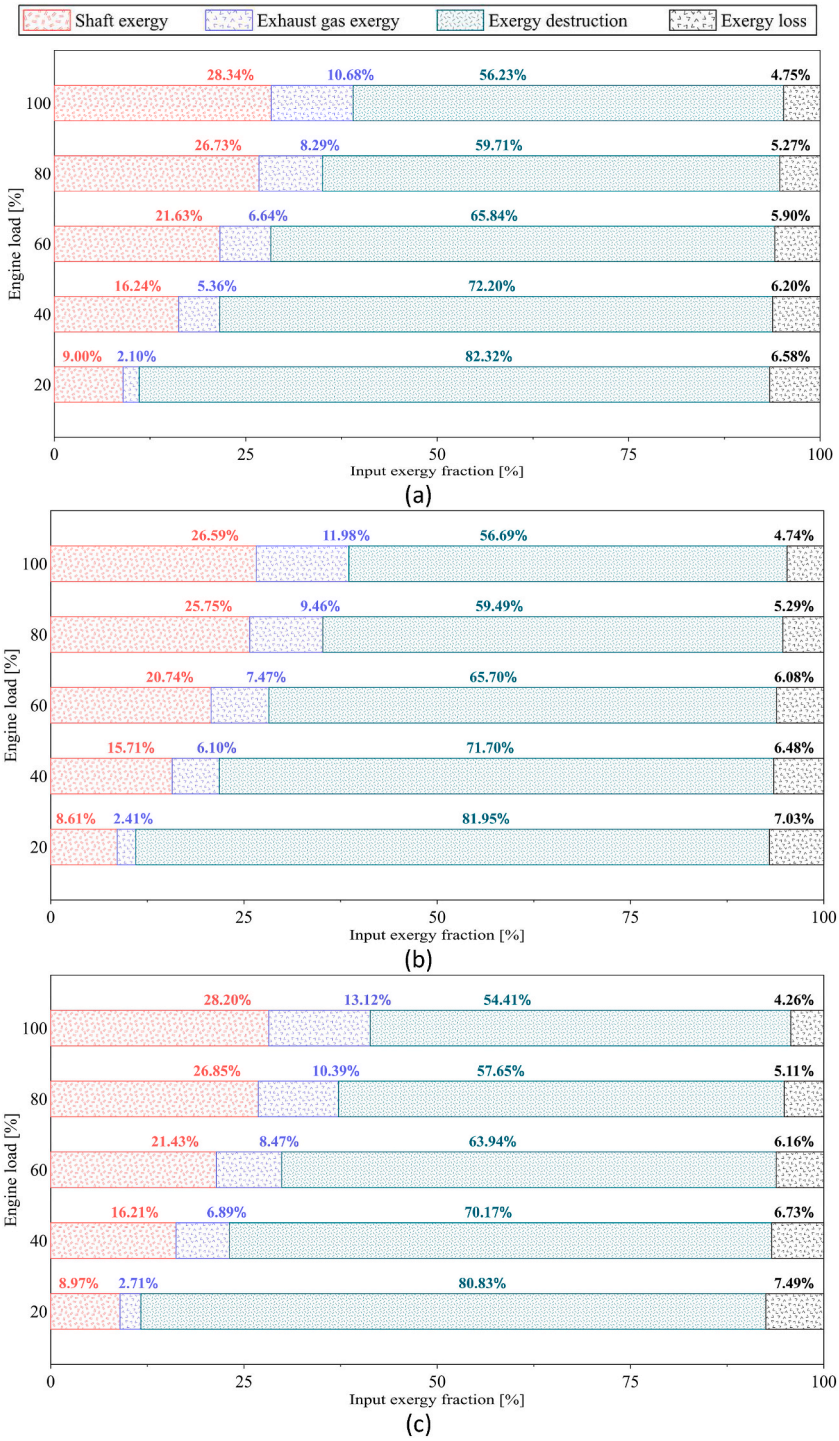

Fig. 5. Exergy distribution for fuel (a) D-100 %, (b) RB-10 % and (c) RB-10 % + H_2(30 %).

rice bran biodiesel causes a 5.58 % increase in CO_2 emissions compared to pure diesel. This is because RB-10 % biodiesel favors the oxidation of the combustion process. The injection of hydrogen into the biodiesel allows for control of the increase in CO_2 emissions. The mixture RB-10 % + H_2(30 %) produces a reduction of 3.71 % compared to rice bran biodiesel. This reduction in CO_2 emissions is directly associated with the absence of carbon molecules in the hydrogen. Studies indicate that adding hydrogen is beneficial for decreasing CO_2 emissions from engines regardless of the fuel source [44].

Fig. 9 shows the variation of hydrocarbon emissions from the engine resulting from incomplete combustion.

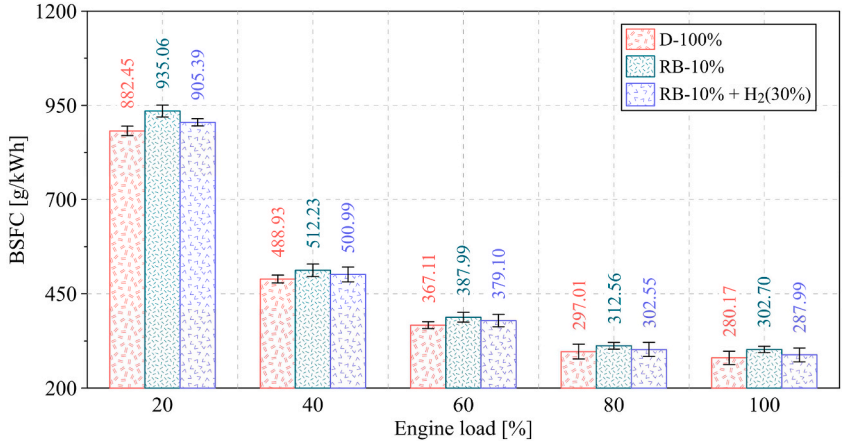

Fig. 6. Variation of BSFC for different fuels.

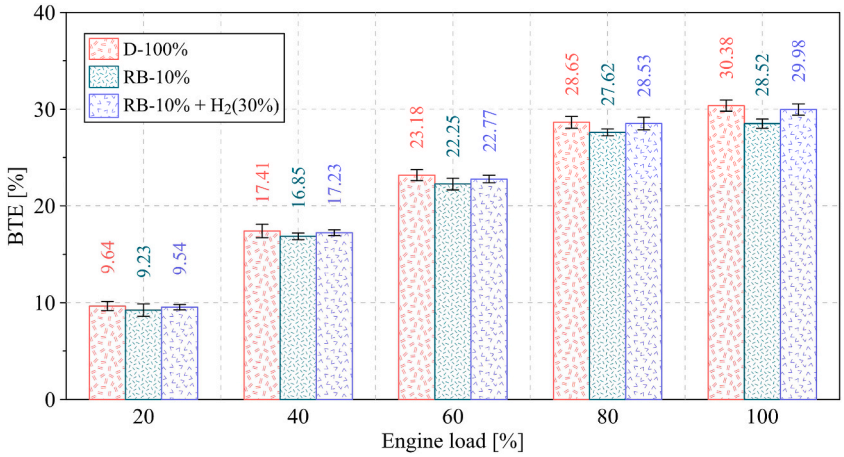

Fig. 7. Variation of BTE for different fuels.

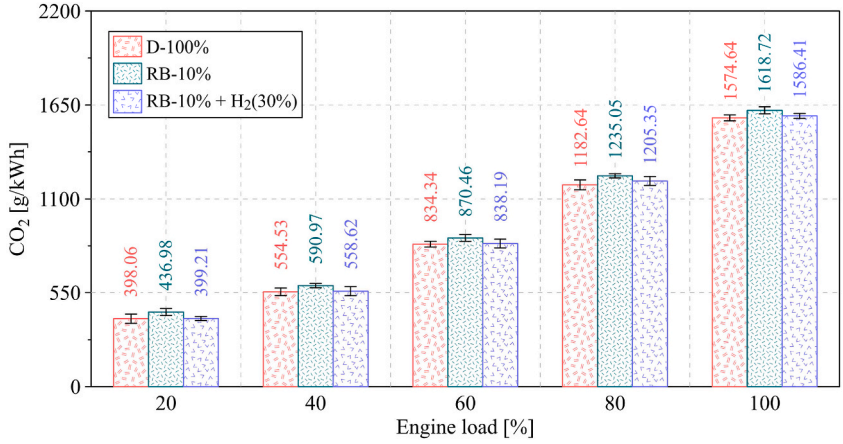

Fig. 8. Variation of CO_2 for different fuels.

The results indicate that RB-10 % and RB-10 % + H_2(30 %) fuels allow a reduction of 5.12 % and 9.90 % in HC emissions compared to pure diesel. The higher oxygen content of rice bran biodiesel, the better homogeneity of the air/fuel mixture, and the increase in combustion temperature are the factors that favor the decrease in HC levels. This is because the increase in temperature promotes

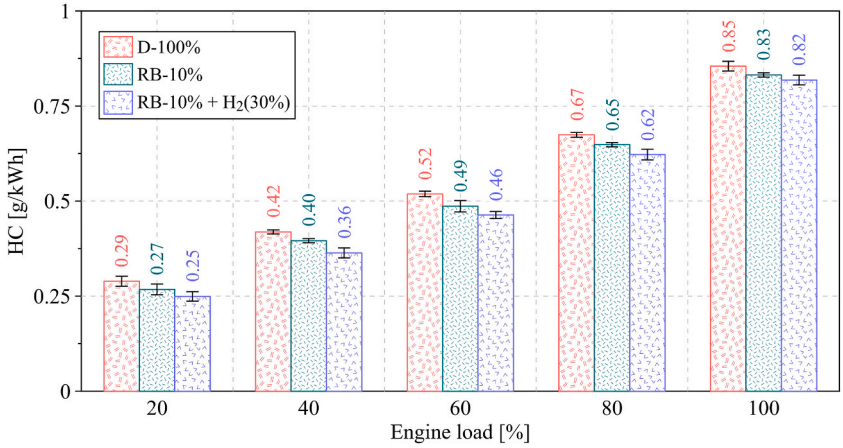

Fig. 9. Variation of HC for different fuels.

oxidation, which reduces the formation of HC emissions. On the other hand, hydrogen does not contain carbon in its chemical composition, and its presence reduces the cooling zones, which also minimizes HC emissions [45,46].

RB-10 % and RB-10 % + H_2(30 %) fuels lead to higher temperature levels inside the combustion chamber, which is a factor favoring nitrogen oxide (NOx) formations. This trend is shown in Fig. 10 for each of the engine load conditions. On average, an increase of 7.60 % and 14.16 % in NOx emissions was obtained using RB-10 % and RB-10 % + H_2(30 %) fuels, respectively. Most studies focused on biodiesel use indicate that NOx emissions are increased because of the excess of oxygen in its molecular structure [47]. The mixture of hydrogen with biodiesel further enhances NOx formation [48].

Carbon monoxide (CO) emissions occur due to incomplete combustion. Fig. 11 shows the variation of CO emissions for the experimental test engine.

Increased engine load tends to result in higher CO emissions for all fuels. However, rice bran biodiesel achieves a 6.08 % decrease in CO emissions when compared to pure diesel. Replacing diesel with rice bran biodiesel reduces CO emissions due to a higher presence of oxygen atoms in the fuel composition, which promotes complete combustion [49]. The decrease in CO formation becomes more evident with hydrogen injection into the biodiesel. The results indicate a 12.57 % reduction with RB-10 % + H2(30 %) mixture. This is a consequence of the higher oxygen content of the biodiesel and the lower percentage of carbon present in the mixture due to the hydrogen. In general, dual-fuel biodiesel-hydrogen engines promote CO oxidation because of higher flame velocity and elevated temperature during combustion. Similar results are reported in the literature [50,51].

RB-10 % and RB-10 % + H_2(30 %) fuels allow for the reduction of the smoke opacity in the engine exhaust gases, as shown in Fig. 12. The results show a decrease of 4.50 % and 10.99 % compared to pure diesel. This implies less soot formation, which is an indication of a more complete combustion in the engine.

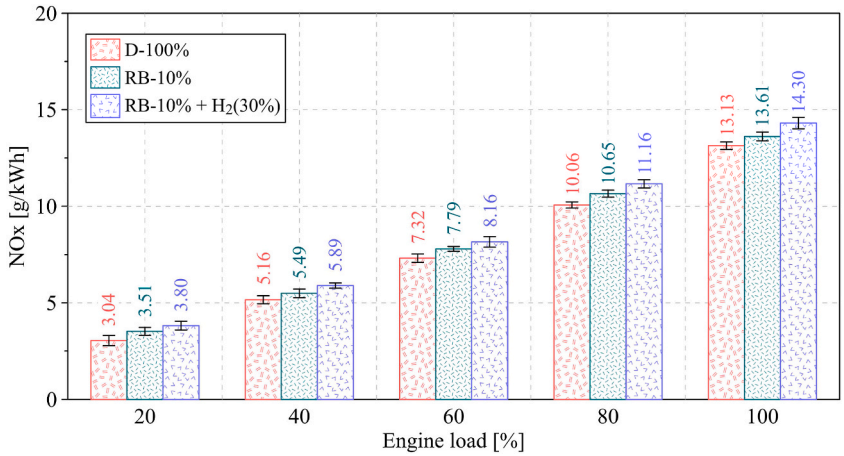

Fig. 10. Variation of NOx for different fuels.

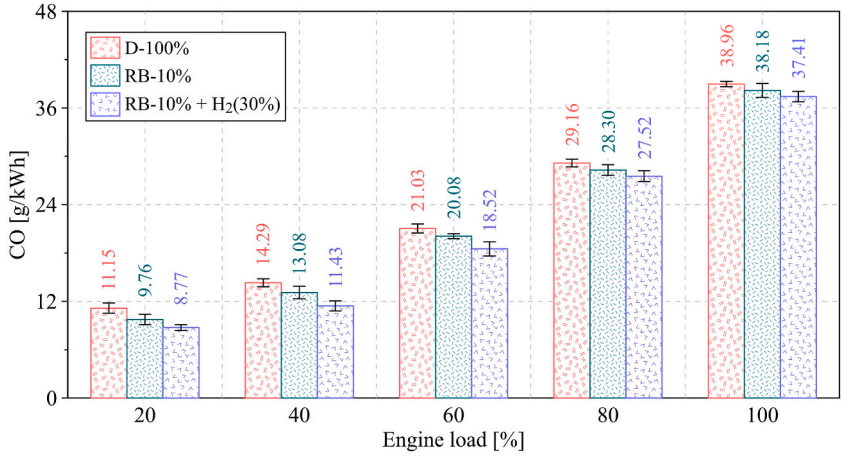

Fig. 11. Variation of CO for different fuels.

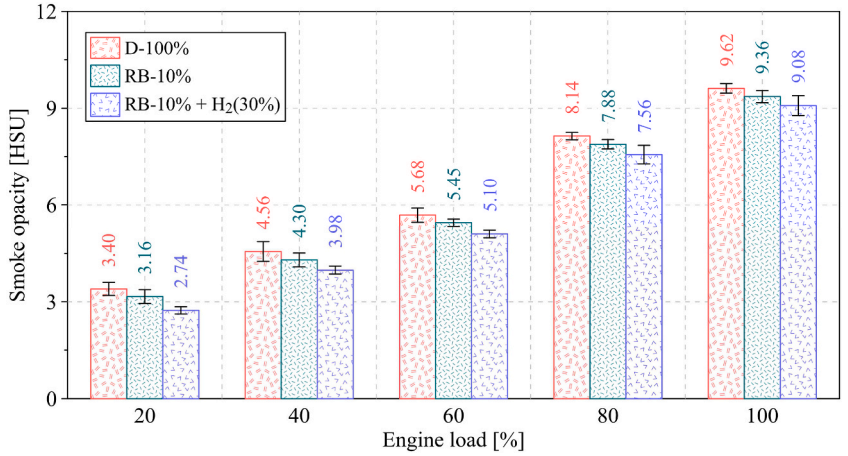

Fig. 12. Variation of smoke opacity for different fuels.

4.5. Operational cost analysis

The operating cost (C_p) was calculated by using the brake specific consumption (BSFC) of the engine, and the operational time (t_p), as shown in equation (14).

$$C_p = BSFC \times \rho_f \times t_p \tag{14}$$

where ρ_f is the fuel price in units of USD/kg. Fig. 13 depicts the trend of the engine operating cost for different fuels and load conditions.

The operational cost refers to the economic cost associated with the price and consumption of fuel, establishing a period of 72 months (6 years). The results obtained indicate that the highest costs occur at the lowest load condition of the engine. This is a direct consequence of the high BSFC and low BTE, which results in high fuel consumption. A maximum cost of 32991 USD/kWh, 34958 USD/kWh, and 33849 USD/kWh are observed for D-100 %, RB-10 %, and RB-10 % + H_2(30 %) fuel, respectively. The operational cost tends to decrease with increasing engine load, reaching an insignificant change for load percentages higher than 80 %.

Rice bran biodiesel causes a 7.42 % increase in operating cost, associated with a higher burn of the RB-10 % fuel to compensate for its lower calorific value. However, the addition of hydrogen in biodiesel allows for the minimization of this situation. The results indicate that the mixture RB-10 % + H_2(30 %) allows a 3.93 % reduction in operating costs compared to RB-10 %.

4.6. Environmental, social, and ecological impact analysis

For the analysis of the environmental, social, and ecological impact, the costs associated with emissions of carbon dioxide, hydrocarbons, nitrogen oxides, and carbon monoxide are considered using Equations (15) and (16).

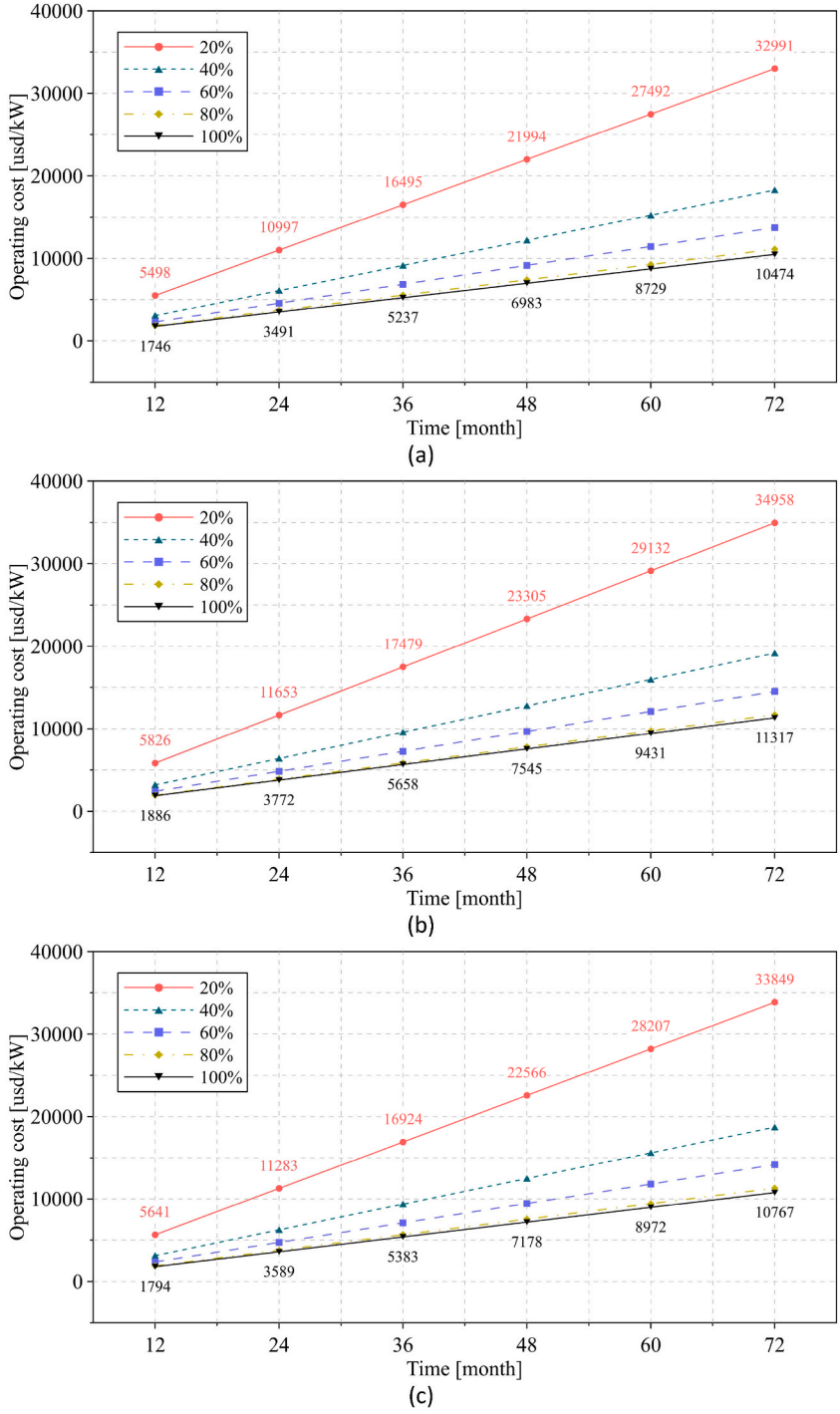

Fig. 13. Variation of operating cost for different fuels: (a) D-100 %, (b) RB-10 %, and (c) RB-10 % + H_2(30 %).

$$ESC_i = \dot{m}_i \times esc_i \tag{15}$$

$$EC_i = \dot{m}_i \times ec_i \tag{16}$$

where ESC_i is the environmental and social impact cost, EC_i is the ecological cost, $\dot{m}_i$ is the flow of pollutant emissions gases. esc_i and ec_i are contants that depend on the type of fuels, whose values are shown in Table 6.

Fig. 14 shows the environmental and social impact cost results obtained for the different load and fuel conditions. The trends

Table 6
Constant for environmental and social impact cost, and ecological cost.

Emissions gases	Unit	Constant	
		Ecological cost	Environmental and social impact cost
CO_2	USD/kg	0.116	0.06
HC	USD/kg	3.538	7.21
CO	USD/kg	0.24	3.63
NOx	USD/kg	6.36	21.63

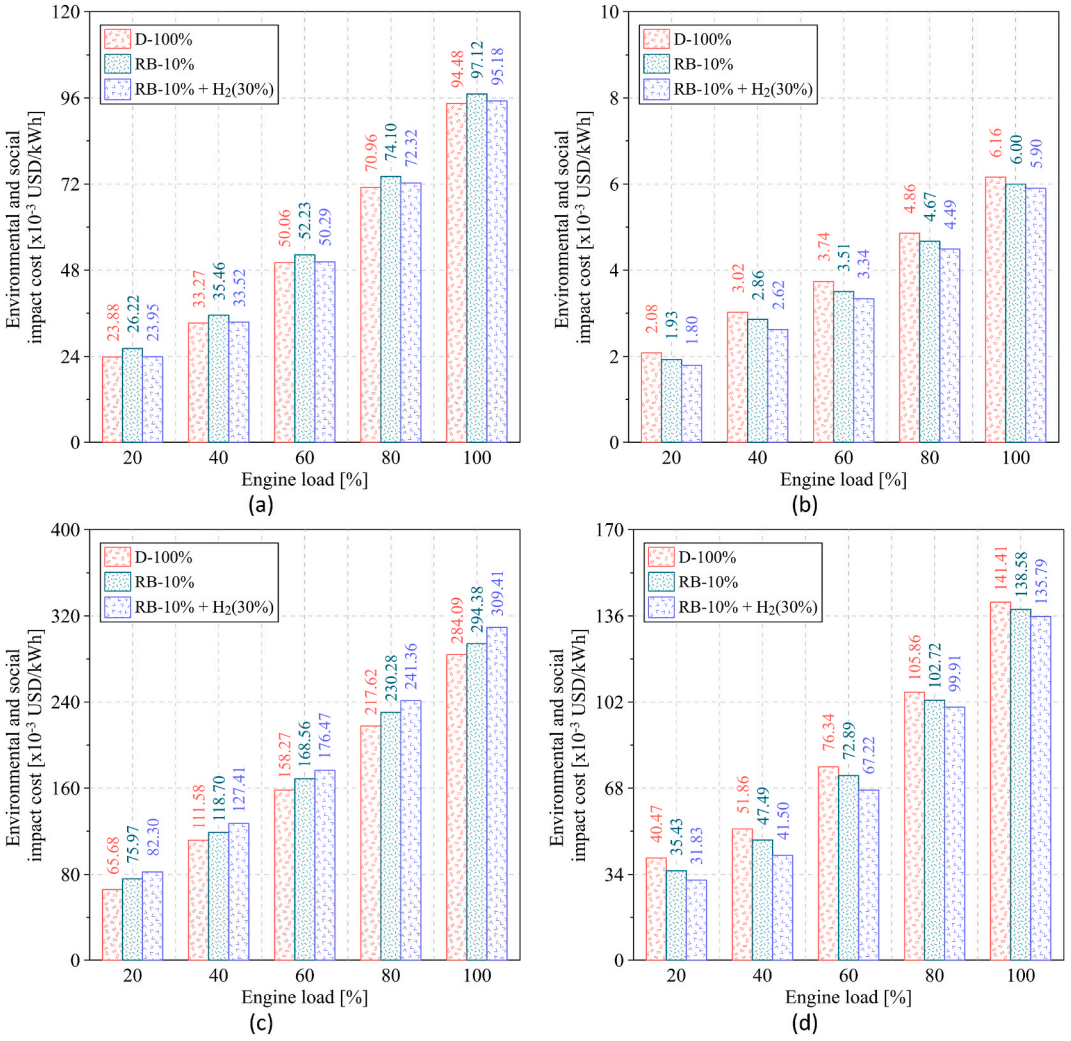

Fig. 14. Environmental and social impact cost for (a) CO_2, (b), HC (c) NOx, and (d) CO.

obtained indicate an increase in environmental and social costs in relation to the engine load. This is a consequence of a higher amount of pollutant emissions in the exhaust gases when the engine operates with a higher mechanical power output. On average, the environmental and social impact cost of CO_2, HC, NOx, and CO emissions tend to increase by 40.46 %, 33.09 %, 41.73 %, and 40.66 % when the engine load is increased by 20 %. Rice bran biodiesel (RB-10 %) reduces 5.12 % and 6.08 % in the environmental and social cost of HC and CO emissions compared to pure diesel. However, this type of biodiesel causes an increase of 5.58 % and 7.60 % in the environmental and social cost of CO_2 and NOx emissions, respectively. Hydrogen injection reduces the environmental and social cost of CO_2, HC, and CO emissions by 4.44 %, 5.07 %, and 7.06 % when comparing the mixture RB-10 % + H_2(30 %) with biodiesel, respectively. Despite the advantages that biodiesel and hydrogen promote, both cause an increase in the environmental and social cost of NOx emissions.

Fig. 15 shows each fuel type's ecological costs for CO2, HC, NOx, and CO emissions. The mixture RB-10 % + H_2(30 %) reduces the

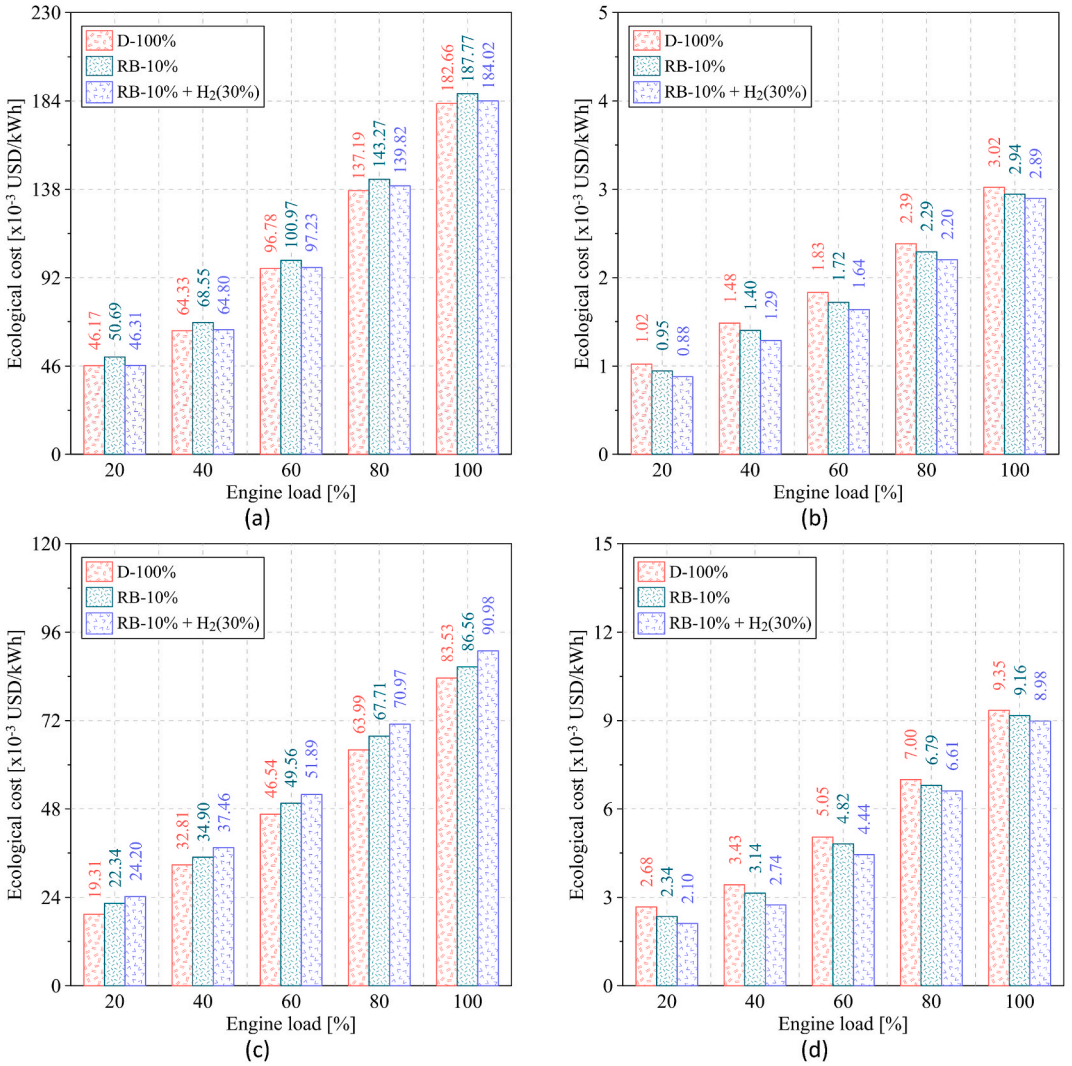

Fig. 15. Ecological cost for (a) CO_2, (b), HC (c) NOx, and (d) CO.

ecological cost of CO2, HC, and CO emissions of 0.83 %, 9.90 %, and 12.57 % compared to pure diesel. Additionally, a decrease of 4.44 %, 5.07 %, and 7.06 % was observed when compared to rice bran biodiesel. The pollutant emissions with the highest ecological cost were NOx, with CO, CO_2, and HC emissions in second, third, and fourth place, respectively. In general, the addition of hydrogen in rice bran biodiesel favors the reduction of the ecological cost of CO_2, HC, and CO emissions.

4.7. Exergoeconomic analysis

For the economic exergy analysis of the engine, the calculation of the cost of useful work (C_w) and the cost of exergy loss (C_ψ) are considered, which were calculated by means of equation (17) and equation (18).

$$C_W = \frac{\left(C_{fuel} \times [\dot{\psi}_s - \dot{\psi}_{exh} - \dot{\psi}_{loss}] \times 3600\right) + \left(\frac{c_f \times e_f \times M_f}{t_p}\right)}{\dot{\psi}_s} \tag{17}$$

$$C_{\dot{\psi}} = \frac{C_{fuel} \times (\dot{\psi}_{loss} + \dot{\psi}_{exh} + \dot{\psi}_{dest}) \times 3600}{\dot{\psi}_s} \tag{18}$$

where C_{fuel} is the price of the fuel, c_f is the engine cost, e_f is the capital factor of the investment, t_p operating time per year, and M_f is the engine maintenance factor, respectively. The price of the fuel (C_{fuel}) and capital factor of the investment (e_f) were calculated using the following equations:

$$C_{fuel} = \frac{\zeta}{\rho \times LHV} \tag{19}$$

$$e_f = \frac{i \times (1+i)^n}{(1+i)^n - 1} \tag{20}$$

where ρ is the density of the fuel, ζ is the price of fuel per cubic meter, n is the engine lifetime, and i is the interest rate. Fig. 16 shows the trend of the cost of useful work and the cost of exergy loss of the engine running on diesel, rice bran biodiesel, and its mixture with hydrogen.

The variation of the cost useful work varies from 0.381 to 1.304 USD/kWh, 0.400–1.351 USD/kWh, and 0.374–1.287 USD/kWh for D-100 %, RB-10 % and RB-10 % + H_2(30 %) fuels, respectively. In general, the lower thermal efficiency and lower calorific value of rice bran biodiesel lead to a 3.18 % increase in the cost of useful work. However, the 30 % hydrogen energy fraction in RB-10 % leads to a 1.88 % and 4.90 % decrease compared to pure diesel and rice bran biodiesel. This is a direct consequence of the high energy contribution of hydrogen in RB-10 %.

The higher levels of exhaust gases exergy and exergy loss present in the rice bran biodiesel cause an increase of 5.74 % in the cost of exergy loss. The maximum values reached were 1.276 USD/kWh, 1.339 USD/kWh, and 1.280 USD/kWh for the D-100 %, RB-10 % and RB-10 % + H_2(30 %) fuels. The mixture of biodiesel and hydrogen allows a 5.08 % reduction in the cost of exergy loss. The decrease is attributed to reduced exergy loss and exergy destruction when the engine runs on hydrogen.

5. Conclusions

The present research evaluated the combustion characteristics, energy and energy balance, performance parameters, emission levels, and operating costs of a diesel engine generator fueled with rice bran biodiesel and hydrogen gas. Five load conditions were considered for the analysis: 20 %, 40 %, 60 %, 80 %, and 100 %, and three types of fuels were used: D-100 %, RB-10 %, and RB-10 % +

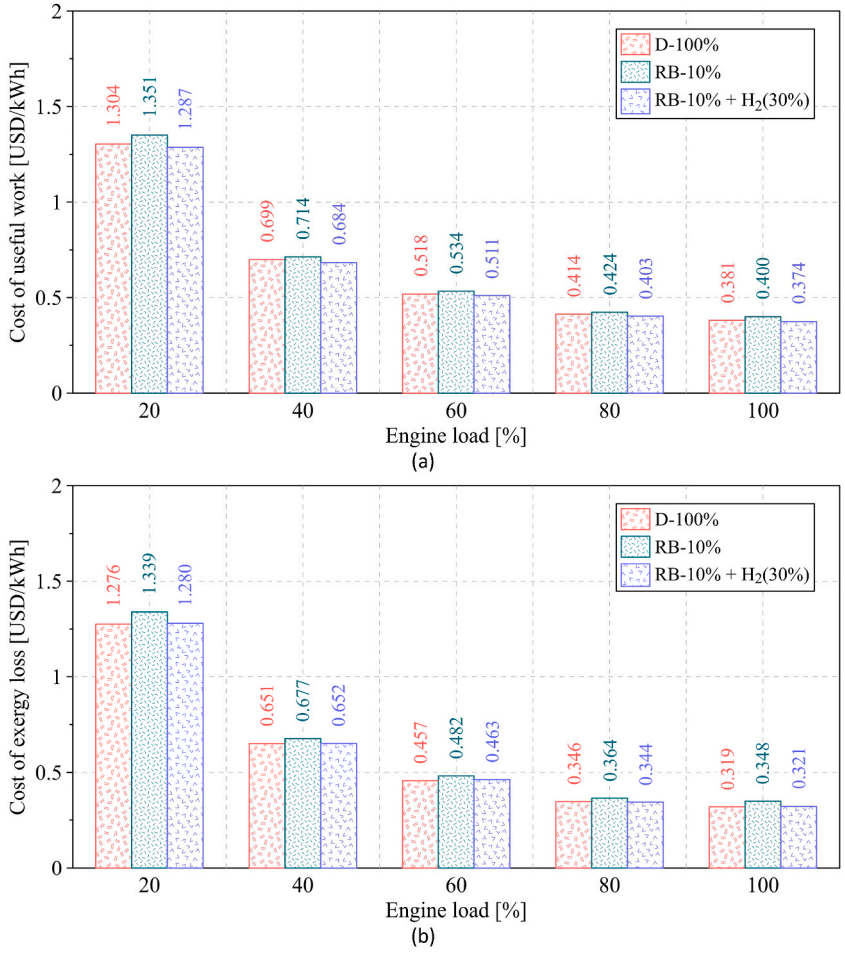

Fig. 16. Exergoeconomic analysis: (a) cost of useful work and (b) cost of exergy loss.

H_2(30 %). The main findings of the research are shown below.

1. The analysis of the combustion characteristics shows that rice bran biodiesel (RB-10 %) reduces the maximum pressure and heat release rate values by 7.80 % and 9.53 % compared to D-100 %. However, with the mixture RB-10 % + H_2(30 %), an increase of 4.05 % and 6.40 % is obtained compared to RB-10 % fuel.
2. The injection of hydrogen into rice bran biodiesel allows a 3.26 % increase in BTE. Furthermore, it is shown that the mixture RB-10 % + H_2(30 %) achieves a 3.14 % reduction in BSFC relative to RB-10 %.
3. The additional oxygen provided by the rice bran biodiesel and the higher homogeneity of the air/fuel mixture due to the hydrogen allows a significant reduction of pollutant emissions from the engine. The results show that the mixture RB-10 % + H_2(30 %) reduces HC, CO, and smoke opacity emissions by 9.90 %, 12.57 %, and 10.99 % compared to pure diesel. In addition, the absence of carbon in the hydrogen minimizes the formation of CO_2 emissions in RB-10 % biodiesel.
4. The mixture RB-10 % + H_2(30 %) leads to a 3.93 % reduction in the operational cost of the engine, compared to RB-10 % fuel. In addition, the mixture RB-10 % + H_2(30 %) allows a reduction in environmental and social impact cost and ecological cost of 4.44 %, 5.07 %, and 7.06 % for CO_2, HC, and CO emissions, to RB-10 % biodiesel. The injection of hydrogen into rice bran biodiesel also results in a 4.90 % and 5.08 % decrease in the cost of useful work and exergy loss.

In general, hydrogen injection is a promising alternative to promote the use of rice bran biodiesel due to its improved performance characteristics and reduced pollutant emissions without requiring engine modifications. Research has shown that the proposed mixture RB-10 % + H2(30 %) performance is considerably similar to pure diesel. Therefore, the analyzed mixture can be used in various economic activities where the diesel engine is present, such as in the transport, industrial, and agricultural sectors, without significantly impacting energy efficiency. The high availability of rice bran in Colombia as a raw material makes it possible to obtain biodiesel at a low economic cost, which favors the reduction of the operational cost of the engine and avoids the presence of waste that can affect the ecosystem.

Data availability

The data used were specified in the manuscript.

CRediT authorship contribution statement

Raquel Laguado-Ramírez: Writing – original draft, Resources, Project administration, Investigation, Formal analysis, Conceptualization. **Fanny Hernandez-Villamizar:** Writing – original draft, Resources, Methodology, Funding acquisition, Conceptualization. **Jorge Duarte-Forero:** Writing – review & editing, Visualization, Validation, Supervision, Resources, Investigation, Formal analysis, Data curation, Conceptualization.

Declaration of competing interest

The authors declare that they have no known competing financial interests or personal relationships that could have appeared to influence the work reported in this paper.

Acknowledgments

The authors want to acknowledge the support of the UNIVERSIDAD DEL ATLÁNTICO and UNIVERSIDAD FRANCISCO DE PAULA SANTANDER on the development of this research.

References

[1] G.V. Ochoa, J.D. Forero, J.P. Rojas, A comparative energy and exergy optimization of a supercritical-CO2 Brayton cycle and Organic Rankine Cycle combined system using swarm intelligence algorithms, Heliyon 6 (2020) e04136.
[2] I.C. Setiawan, M. Setiyo, Renewable and sustainable green diesel (D100) for achieving net zero emission in Indonesia transportation sector, automot, Exp. 5 (2022) 1–2.
[3] G. Wu, D. Wu, Y. Li, L. Meng, others, effect of acetone-n-butanol-ethanol (ABE) as an oxygenate on combustion, performance, and emission characteristics of a spark ignition engine, J. Chem. 2020 (2020).
[4] D. Han, E. Jiaqiang, Y. Deng, J. Chen, E. Leng, G. Liao, X. Zhao, C. Feng, F. Zhang, A review of studies using hydrocarbon adsorption material for reducing hydrocarbon emissions from cold start of gasoline engine, Renew. Sustain. Energy Rev. 135 (2021) 110079.
[5] D. Maestre-Cambronel, J. Guzmán Barros, A. Gonzalez-Quiroga, A. Bula, J. Duarte-Forero, Thermoeconomic analysis of improved exhaust waste heat recovery system for natural gas engine based on Vortex Tube heat booster and supercritical CO2 Brayton cycle, Sustain. Energy Technol. Assessments 47 (2021) 101355–101371.
[6] M.A. Ruhul, M.J. Abedin, S.M.A. Rahman, B.H.H. Masjuki, A. Alabdulkarem, M.A. Kalam, I. Shancita, Impact of fatty acid composition and physicochemical properties of Jatropha and Alexandrian laurel biodiesel blends: an analysis of performance and emission characteristics, J. Clean. Prod. 133 (2016) 1181–1189.
[7] L. Fan, F. Cheng, T. Zhang, G. Liu, J. Yuan, P. Mao, Visible-light photoredox-promoted desilylative allylation of a-silylamines: an efficient route to synthesis of homoallylic amines, Tetrahedron Lett. 81 (2021) 153357.
[8] O.M. Ali, R. Mamat, N.R. Abdullah, A.A. Abdullah, Analysis of blended fuel properties and engine performance with palm biodiesel–diesel blended fuel, Renew. Energy 86 (2016) 59–67.

[9] M.P. Dorado, E. Ballesteros, J.M. Arnal, J. Gomez, F.J. Lopez, Exhaust emissions from a Diesel engine fueled with transesterified waste olive oil, Fuel 82 (2003) 1311–1315.
[10] G. Ergen, Comprehensive analysis of the effects of alternative fuels on diesel engine performance combustion and exhaust emissions: role of biodiesel, diethyl ether, and EGR, Therm. Sci. Eng. Prog. 47 (2024) 102307.
[11] A.N. Phan, T.M. Phan, Biodiesel production from waste cooking oils, Fuel 87 (2008) 3490–3496.
[12] A. Cernat, C. Pana, N. Negurescu, G. Lazaroiu, C. Nutu, The influence of hydrogen on vaporization, mixture formation and combustion of diesel fuel at an automotive diesel engine, Sustainability 13 (2020) 202.
[13] O.M.I. Nwafor, Effect of choice of pilot fuel on the performance of natural gas in diesel engines, Renew. Energy 21 (2000) 495–504.
[14] V. Gnanamoorthi, V.T. Vimalananth, Effect of hydrogen fuel at higher flow rate under dual fuel mode in CRDI diesel engine, Int. J. Hydrogen Energy 45 (2020) 16874–16889.
[15] A. Jamrozik, K. Grab-Rogaliński, W. Tutak, Hydrogen effects on combustion stability, performance and emission of diesel engine, Int. J. Hydrogen Energy 45 (2020) 19936–19947.
[16] A. Mej\'\ia, M. Leiva, A. Rincón-Montenegro, A. Gonzalez-Quiroga, J. Duarte-Forero, Experimental assessment of emissions maps of a single-cylinder compression ignition engine powered by diesel and palm oil biodiesel-diesel fuel blends, Case Stud. Therm. Eng. 19 (2020) 100613.
[17] D. Mendoza-Casseres, G. Valencia-Ochoa, J. Duarte-Forero, Experimental assessment of combustion performance in low-displacement stationary engines operating with biodiesel blends and hydroxy, Therm. Sci. Eng. Prog. 23 (2021) 100883–100896.
[18] J. Duarte-Forero, D. Mendoza-Casseres, G. Valencia-Ochoa, Energy, Exergy, and emissions (3E) assessment of a low-displacement engine powered by biodiesel blends of palm oil mill effluent (POME) and hydroxy gas, Therm. Sci. Eng. Prog. 26 (2021) 101126–101141.
[19] M. Loganathan, V.M. Madhavan, K.A. Balasubramanian, V. Thanigaivelan, M. Vikneswaran, A. Anbarasu, Investigation on the effect of diethyl ether with hydrogen-enriched cashew nut shell (CNS) biodiesel in direct injection (DI) diesel engine, Fuel 277 (2020) 118165.
[20] M.A. Akar, E. Kekilli, O. Bas, S. Yildizhan, H. Serin, M. Ozcanli, Hydrogen enriched waste oil biodiesel usage in compression ignition engine, Int. J. Hydrogen Energy 43 (2018) 18046–18052.
[21] K. Winangun, A. Setiyawan, B. Sudarmanta, The combustion characteristics and performance of a Diesel Dual-Fuel (DDF) engine fueled by palm oil biodiesel and hydrogen gas, Case Stud. Therm. Eng. (2023) 102755.
[22] X. Zhang, H. Li, M. Sekar, M. Elgendi, N.R. Krishnamoorthy, C. Xia, D.P. Matharasi, Machine learning algorithms for a diesel engine fuelled with biodiesel blends and hydrogen using LSTM networks, Fuel 333 (2023) 126292.
[23] R. Jayabal, Effect of hydrogen/sapota seed biodiesel as an alternative fuel in a diesel engine using dual-fuel mode, Process Saf. Environ. Protect. 183 (2024) 890–900.
[24] D. Tan, Y. Wu, J. Lv, J. Li, X. Ou, Y. Meng, G. Lan, Y. Chen, Z. Zhang, Performance optimization of a diesel engine fueled with hydrogen/biodiesel with water addition based on the response surface methodology, Energy 263 (2023) 125869.
[25] A. Mohite, B.J. Bora, Ü. Augbulut, P. Sharma, B.J. Medhi, D. Barik, Optimization of the pilot fuel injection and engine load for an algae biodiesel-hydrogen run dual fuel diesel engine using response surface methodology, Fuel 357 (2024) 129841.
[26] E.M. Vargas, M. Aguirre, El salvado de arroz: procesos de estabilización y usos potenciales en la industria colombiana, 2011. Bogotá.
[27] Y.A. Rodriguez-Restrepo, P. Ferreira-Santos, C.E. Orrego, J.A. Teixeira, C.M.R. Rocha, Valorization of rice by-products: protein-phenolic based fractions with bioactive potential, J. Cereal. Sci. 95 (2020) 103039.
[28] Claudia Liliana Lozano Rojas, Alternativas de usos de la cascarilla de arroz (Oriza sativa) en Colombia para el mejoramiento del sector productivo y la industria, Universidad Nacional Abierta y a Distancia - UNAD, 2020.
[29] S. Thiyagarajan, E. Varuvel, V. Karthickeyan, A. Sonthalia, G. Kumar, C.G. Saravanan, B. Dhinesh, A. Pugazhendhi, Effect of hydrogen on compression-ignition (CI) engine fueled with vegetable oil/biodiesel from various feedstocks: a review, Int. J. Hydrogen Energy (2022), https://doi.org/10.1016/j.ijhydene.2021.12.147.
[30] S. Kanth, S. Debbarma, B. Das, Experimental investigation of rice bran biodiesel with hydrogen enrichment in diesel engine, Energy Sources, Part A Recover, Util. Environ. Eff. (2020) 1–18.
[31] S. Kanth, T. Ananad, S. Debbarma, B. Das, Effect of fuel opening injection pressure and injection timing of hydrogen enriched rice bran biodiesel fuelled in CI engine, Int. J. Hydrogen Energy 46 (2021) 28789–28800.
[32] M.K. Yesilyurt, A detailed investigation on the performance, combustion, and exhaust emission characteristics of a diesel engine running on the blend of diesel fuel, biodiesel and 1-heptanol (C7 alcohol) as a next-generation higher alcohol, Fuel 275 (2020) 117893.
[33] G. Valencia, J. Núñez, J. Duarte, Multiobjective optimization of a plate heat exchanger in a waste heat recovery organic rankine cycle system for natural gas engines, Entropy 21 (2019) 655–675.
[34] G.A. Diaz, J.D. Forero, J. Garcia, A. Rincon, A. Fontalvo, A. Bula, R.V. Padilla, Maximum power from fluid flow by applying the first and second laws of thermodynamics, J. Energy Resour. Technol. 139 (2017) 032903.
[35] G.V. Ochoa, C. Isaza-Roldan, J.D. Forero, A phenomenological base semi-physical thermodynamic model for the cylinder and exhaust manifold of a natural gas 2-megawatt four-stroke internal combustion engine, Heliyon 5 (2019) e02700.
[36] G. Valencia Ochoa, C. Acevedo Peñaloza, J. Duarte Forero, Thermoeconomic optimization with PSO algorithm of waste heat recovery systems based on organic rankine cycle system for a natural gas engine, Energies 12 (2019) 1–21.
[37] I. Glassman, Combustion Academic, Press Inc, 1987.
[38] G. Woschni, A universally applicable equation for the instantaneous heat transfer coefficient in the internal combustion engine, SAE Trans. 670931 (1968) 3065–3083.
[39] P. Lyubarskyy, D. Bartel, 2D CFD-model of the piston assembly in a diesel engine for the analysis of piston ring dynamics, mass transport and friction, Tribol. Int. 104 (2016) 352–368.
[40] J.M. Díaz, Aportación al diagnóstico de la combustión en motores Diésel de inyección directa, Universitat Politècnica de València, 2007.
[41] P. Chelladorai, E.G. Varuvel, L.J. Martin, N. Bedhannan, Synergistic effect of hydrogen induction with biofuel obtained from winery waste (grapeseed oil) for CI engine application, Int. J. Hydrogen Energy 43 (2018) 12473–12490.
[42] G. Dhamodaran, R. Krishnan, Y.K. Pochareddy, H.M. Pyarelal, H. Sivasubramanian, A.K. Ganeshram, A comparative study of combustion, emission, and performance characteristics of rice-bran-, neem-, and cottonseed-oil biodiesels with varying degree of unsaturation, Fuel 187 (2017) 296–305.
[43] V.E. Geo, C. Prabhu, S. Thiyagarajan, T. Maiyalagan, F. Aloui, Comparative analysis of various techniques to improve the performance of novel wheat germ oil–an experimental study, Int. J. Hydrogen Energy 45 (2020) 5745–5756.
[44] E. Uludamar, Effect of hydroxy and hydrogen gas addition on diesel engine fuelled with microalgae biodiesel, Int. J. Hydrogen Energy 43 (2018) 18028–18036.
[45] M.A. Rahman, A.M. Ruhul, M.A. Aziz, R. Ahmed, Experimental exploration of hydrogen enrichment in a dual fuel CI engine with exhaust gas recirculation, Int. J. Hydrogen Energy 42 (2017) 5400–5409, https://doi.org/10.1016/j.ijhydene.2016.11.109.
[46] Z. Zhang, H. Liu, Y. Li, Y. Ye, J. Tian, J. Li, Y. Xu, J. Lv, Research and optimization of hydrogen addition and EGR on the combustion, performance, and emission of the biodiesel-hydrogen dual-fuel engine with different loads based on the RSM, Heliyon 10 (2024) e23389.
[47] V. Karthickeyan, B. Ashok, K. Nanthagopal, S. Thiyagarajan, V.E. Geo, Investigation of novel Pistacia khinjuk biodiesel in DI diesel engine with post combustion capture system, Appl. Therm. Eng. 159 (2019) 113969.
[48] G. Tüccar, Experimental study on vibration and noise characteristics of a diesel engine fueled with mustard oil biodiesel and hydrogen gas mixtures, Biofuels 12 (5) (2018) 537–542.

[49] A. Datta, B.K. Mandal, A comprehensive review of biodiesel as an alternative fuel for compression ignition engine, Renew. Sustain. Energy Rev. 57 (2016) 799–821.
[50] H. Serin, S. Yildizhan, Hydrogen addition to tea seed oil biodiesel: performance and emission characteristics, Int. J. Hydrogen Energy 43 (2018) 18020–18027.
[51] Z. Zhang, S. Wang, M. Pan, J. Lv, K. Lu, Y. Ye, D. Tan, Utilization of hydrogen-diesel blends for the improvements of a dual-fuel engine based on the improved Taguchi methodology, Energy 292 (2024) 130474.